Improved Beamspace MUSIC for Finding Directions of BPSK and QPSK Coherent Arrivals

RAUNGRONG SULEESATHIRA and NAVAPOL PHAISAL-ATSAWASENEE
Department of Electronic and Telecommunication Engineering, Faculty of Engineering
King Mongkut's University of Technology Thonburi
126 Pracha-utis Rd., Bangmod, Tungkru, Bangkok 10140
THAILAND
raungrong.sul@kmutt.ac.th

Abstract: - Coherence is often encountered in sonar, radar or mobile communications. Performance of the beamspace MUSIC (MUltiple Signal Classification) deteriorates as coherent arrivals become closely space. An improvement for the beamspace MUSIC resolution is presented. Decorrelation as a preprocessing is performed by the techniques called forward-backward spatial smoothing. Based on the fact that signal eigenvectors of the smoothed correlation matrix of the received signals contains the DOA vectors, combining all signal eigenvectors into a signal sequence enable us to obtain estimated DOAs. This combined signal eigenvector is equivalent to an array output impinged by the partially correlated sources. As a consequence, forward-backward averaging is presented to decorrelate the coherence in the correlation matrix of the combined signal eigenvector before applying the beamspace MUSIC to extract the DOA information. Evaluations are given to illustrate the capability of the proposed method to distinguish closely spaced directions and reduce estimation errors in the presence of fully correlation. Performance analysis of BPSK and QPSK modulations are derived and compared with the simulation results.

Key-Words: - Antenna array, Beamforming, Coherent sources, Digital communication, Direction of Arrival

1 Introduction

Application of the antenna array for direction finding or source localization has been interested in sonar, radar especially in spatial division multiple access (SDMA) used in mobile communications [1]. Subspace-based methods such as element space MUSIC, beamspace MUSIC, ESPRIT and MinNorm are efficient to estimate directions of arrival (DOAs) utilizing a task of space-time processing. Except for the reduction of computation, the beamspace MUSIC has several advantages compared with the element space MUSIC in small samples such as reduced sensitivity of system errors, reduced resolution threshold, reduced bias in estimates, increased probabilities of resolution [2], [3]. Therefore, it is of interest to exploit the beamspace processing for the DOA estimation. However, the main limitation of such subspace-based method is that it performs poorly in the presence of highly correlated and coherent (perfectly correlated) incoming signals. A number of high resolution direction finding approaches have been proposed to improve the resolution of the beamspace MUSIC for coherent sources [4]-[11].

To decorrelate, the forward-backward spatial smoothing [4] is presented as a preprocessor of the beamspace MUSIC. Smoothed correlation matrix can recover the reduced rank of the covariance matrix due to the coherence of signal sources [5], [6]. The recovered rank is needed to be equal to the number of signals impinging on the antenna array. In [5], the DOAs that are shown in the simulation results are not very close which are between $10^\circ - 13^\circ$. The method called the quadratic spatial smoothing technique [6] by squaring the array covariance matrix before forming the smoothed covariance matrix can improve the resolution of coherent signals. Constrain beamspace MUSIC in [7] assumes that some of the signal directions are priori known precisely and some of them are known approximately. This can reduce the variance of DOA estimation error. In [8], designing a beamformer is introduced to enhance the resolution performance of the beamspace MUSIC. The approach constructs the beamforming matrix to maximize the metric for a selected cluster. As a result, the performance depends on the cluster selection. An analysis of a beamspace version of the MUSIC algorithm applicable to two closely spaced emitters in diverse scenarios is given in [9]. The approach presented in [10] is a modified beamspace MUSIC algorithm for high resolution array processing. However, an appropriate prior knowledge of the source localization sectors is still required and the algorithm needs more computations than the conventional beamspace MUSIC. When a subset of the sources is found to be coherent, an iterative method given to estimate azimuth-elevation angles is high complex [11]. The coarse and fine estimation can make the beamspace MUSIC have high-speed DOA estimation [12]. A high resolution DOA estimation approach for coherent/noncoherent sources is based on the fact that signal eigenvectors of the covariance matrix are a linear combination of steering vector [13]. Correspondingly, employing the benefits of the technique of the forward-backward spatial smoothing and the signal eigenvector would result in an improvement of the beamspace MUSIC.

This paper is organized as follows. It begins with a correlated signal model in section 2. Then, an overview of the beamspace MUSIC is given in section 3. Section 4 describes the forward-backward spatially smoothing. Combined signal eigenvector is explained in section 5. An algorithm to improve angular resolution of beamspace MUSIC is proposed in section 6. In section 7, its application to BPSK (Binary Phase Shift Keying) and QPSK (Quadrature Phase Shift Keying) coherent arrivals are shown to derive expressions of probability of bit errors and probability of symbol errors. Simulation results to illustrate the performance are presented in section 8 followed by conclusion in section 9.

2 Correlated Signal Model

Consider a linear array of L omnidirectional elements. In far field, two sinusoidal sources consists of signal source, $m_s(n)$, and interference $m_i(n)$. Let p_s and p_i represent power of the signal source and the interference, respectively. Define an $L\times 1$ dimensional vector $\mathbf{x}(n)$ to represent L waveform outputs from the L elements of the array at time n as [2]

$$\mathbf{x}(n) = \sqrt{p_s}\, m_s(n)\mathbf{a}(\theta_s) + \sqrt{p_i}\left(\delta^* m_s(n) + \sqrt{1-|\delta|^2}\, m_i(n)\right)\mathbf{a}(\theta_i) + \mathbf{n}(n) \quad (1)$$

where a complex scalar δ represents the correlation coefficients between the two sources. The vectors $\mathbf{a}(\theta_s)$ and $\mathbf{a}(\theta_i)$ are steering vectors in the directions of arrival θ_s and θ_i, respectively, given by [14]

$$a(\theta) = \begin{bmatrix} 1 & e^{-j2\pi\frac{d}{\lambda}\sin\theta} & \dots & e^{-j2\pi\frac{d}{\lambda}(L-1)\sin\theta} \end{bmatrix}^T_{L\times 1}. \quad (2)$$

Let θ_s be the DOA of the signal source while θ_i be the DOA of the interference. We use $d = 0.5\lambda$. That is the element spacing d is a half of wavelength λ. The vector $\mathbf{n}(n)$ represents Gaussian noise vector with zero mean and variance σ_n^2 on each antenna element which is the temporal narrowband spectrum and spatially white spectrum. The operator * denotes the complex conjugate and superscript T denotes the transpose operation. Note that the value δ indicates the quantity of the correlation field. When $|\delta| = 1$, the two sources are coherent with their fixed phase difference. If $|\delta| < 1$, the two sources are partially correlated. For $\delta = 0$, there is no correlation between such two sources.

Equation (1) can be written in a matrix form as

$$\mathbf{x}(n) = \mathbf{A}\mathbf{s}(n) + \mathbf{n}(n) \quad (3)$$

where the steering matrix $\mathbf{A}$ can be expressed as

$$\mathbf{A} = [\mathbf{a}(\theta_s) \quad \mathbf{a}(\theta_i)]_{L\times 2} \quad (4)$$

and the vector of coherent sources is

$$\mathbf{s}(n) = \begin{bmatrix} \sqrt{p_s}\, m_s(n) \\ \sqrt{p_i}\left(\delta m_s(n) + \sqrt{1-|\delta|^2}\, m_i(n)\right) \end{bmatrix}. \quad (5)$$

The array correlation matrix $\mathbf{R}_x$ can be expressed as

$$\mathbf{R_x} = E[\mathbf{x}(n)\mathbf{x}^H(n)]. \quad (6)$$

Substituting Eq. (3) into Eq. (6), this yields

$$\mathbf{R_x} = \mathbf{A}\mathbf{R_s}\mathbf{A}^H + \sigma_n^2\mathbf{I} \quad (7)$$

where $\mathbf{R_s} = E[\mathbf{s}(n)\mathbf{s}^H(n)]$. The superscript H denotes the complex conjugate transposition of a vector or a matrix. In practice, the array correlation matrix can be estimated as $\mathbf{R_x} = \sum_n \mathbf{x}(n)\mathbf{x}^H(n)$ as an average of signal samples.

3 Beamspace MUSIC

In the beamspace MUSIC [5], beamforming is a preprocessor prior to the element-space MUSIC as shown in Fig. 1. The preprocessor generates B beams for the received signal by

$$y(n) = \mathbf{W}^H \mathbf{x}(n) \tag{8}$$

where $\mathbf{W}$ is an $L \times B$ beamforming matrix with $B < L$. The columns form beams toward B expected directions. Using the conventional beamformer [2], each column of matrix $\mathbf{W}$ is defined as

$$\mathbf{w}_b = \frac{1}{L}\mathbf{a}(\theta_b) \qquad b = 1, 2, \ldots, B \tag{9}$$

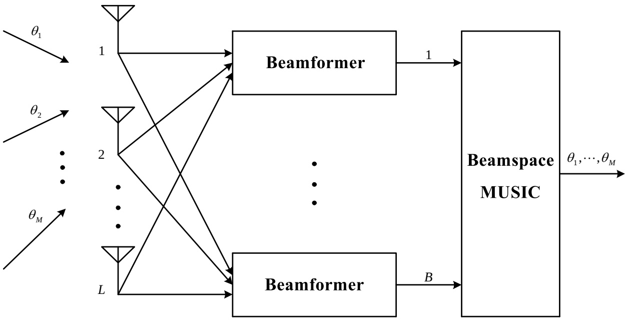

Fig. 1 Beamspace MUSIC

The $B \times B$ beamspace covariance matrix is given by

$$\mathbf{R}_y = \mathbf{W}^H \mathbf{R}_\mathbf{x} \mathbf{W} \tag{10}$$

which can be represented in term of eigenvalues (μ_i) and eigenvectors ($\mathbf{u}_i$) as

$$\begin{aligned}\mathbf{R}_y &= \sum_{i=1}^{B} \mu_i \mathbf{u}_i \mathbf{u}_i^H \\ &= \sum_{i=1}^{M} \mu_i \mathbf{u}_i \mathbf{u}_i^H + \sum_{i=M+1}^{B} \mu_i \mathbf{u}_i \mathbf{u}_i^H\end{aligned} \tag{11}$$

where M is the number of sources. According to Eq. (11), the beamspace covariance matrix is a sum of the signal subspace $\mathbf{S} = [\mathbf{u}_1, \ldots, \mathbf{u}_M]$ and the noise subspace $\mathbf{N} = [\mathbf{u}_{M+1}, \ldots, \mathbf{u}_B]$. Due to the orthogonality between the steering vector and the noise subspace, the beamspace MUSIC can form a spatial spectrum as

$$P(\theta) = \left|\mathbf{a}^H(\theta)\mathbf{W}\mathbf{N}\right|^{-2}. \tag{12}$$

The DOA estimates are located at the peaks of $P(\theta)$. However, the beamspace MUSIC algorithm can fail if sources are coherent. By applying the forward-backward spatial smoothing method before the preprocessed beamforming, the correlation effects can be alleviated.

4 Forward-Backward Spatial Smoothing

Signal correlation can occur when a source is arriving from different DOAs. On the other word, two directional signals are said to be fully correlated or coherent when one is delayed and scaled version of the other. This correlation limits the applicability of the beamspace MUSIC method due to the rank of $\mathbf{R}_y$ is reduced. To restore the rank of the beamspace covariance matrix, decorrelation can be achieved by the forward-backward spatial smoothing method.

To remove the signal correlation, the L element antenna array is divided into K subarrays of size L_0 such that the first subarray consists of Element 1 to Element L_0, the second one consists of Element 2 to Element L_0+1 and so on as shown in Fig. 2. To keep K subarrays of size L_0, one needs $L_0 = L - K + 1$ elements/subarray. In Fig. 2, the arrow directions to the right side indicate the forward smoothing while the left direction is for the backward smoothing.

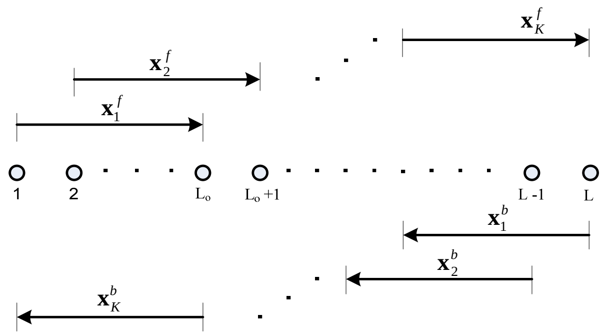

Fig. 2 Forward and backward subarrays

The output of the k^{th} forward subarray is denoted by [2], [4], [5]

$$\mathbf{x}_k^f(n) = \begin{bmatrix} x_k(n) & x_{k+1}(n) & \ldots & x_{k+L_0+1}(n) \end{bmatrix}_{L_0 \times 1}^T \tag{13}$$

and the output of the k^{th} backward subarray is denoted by

$$\mathbf{x}_k^b(n) = \left[x_{L-k+1}^*(n) \;\; x_{L-k}^*(n) \;\; \dots \;\; x_{L-k-L_0+2}^*(n)\right]_{L_0\times 1}^T \quad (14)$$

for $k = 1,\dots,K$. An $L_0 \times L_0$ forward-backward spatially smoothed matrix $\mathbf{R}_\mathbf{x}^{fb}$ can be calculated as

$$\mathbf{R}_\mathbf{x}^{fb} = \frac{1}{KN}\sum_{n=0}^{N-1}\sum_{k=1}^{K}\left[\mathbf{x}_k^f(n)\mathbf{x}_k^{f^H}(n) + \mathbf{x}_k^b(n)\mathbf{x}_k^{b^H}(n)\right] \quad (15)$$

for N snapshots. Substituting $\mathbf{R}_\mathbf{x}^{fb}$ into $\mathbf{R}_\mathbf{x}$ of Eq. (10), it allows us to apply the beamspace MUSIC algorithm to estimate DOAs of coherent arrivals. Besides the beamspace MUSIC scheme, we can extract DOA information using eigenvectors of $\mathbf{R}_\mathbf{x}^{fb}$ as described in the next section.

5 Combined Signal Eigenvectors

In [13], it is shown that each signal eigenvector of the covariance matrix is a linear combination of the direction vectors. Therefore, combining all signal eigenvectors into a single vector enables to estimate the DOAs from this combined signal eigenvector. The signal eigenvector can be combined as

$$\mathbf{c} = \sum_{i=1}^{M} a_i \mathbf{e}_i \quad (16)$$

where $\mathbf{e}_i$ is an eigenvector of $\mathbf{R}_\mathbf{x}^{fb}$ corresponding to one of the M largest eigenvalues (λ_i). The weights are calculated by

$$a_i = \sqrt{\lambda_i - \hat{\sigma}_n^2} \qquad i = 1,2,\dots,M \;. \quad (17)$$

The estimated variance noise is

$$\hat{\sigma}_n^2 = \frac{1}{L_0 - M}\sum_{i=M+1}^{L_0}\lambda_i \quad (18)$$

which depends on the $L_0 - M$ smallest eigenvalues of $\mathbf{R}_\mathbf{x}^{fb}$. Equation (16) can be viewed as an array output as same as Eq. (1) since these equations contains the DOA information. As a result, we can apply a subspace method (e.g. MUSIC) to the combined signal eigenvectors to extract DOA information.

6 Improved Beamspace MUSIC

In this section, we presented an algorithm to improve angular resolution of the beamspace MUSIC in order to estimate DOAs of coherent arrivals. The procedure presented in Fig. 3 performs the following steps.

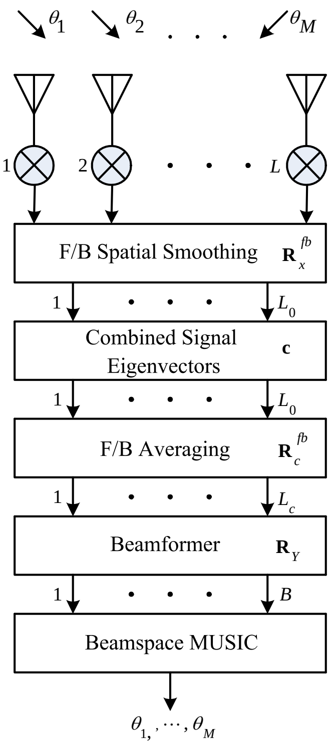

Fig. 3 Improved Beamspace MUSIC

1) Forward-backward spatial smoothing to obtain a decorrelated correlation matrix $\mathbf{R}_\mathbf{x}^{fb}$.
2) Find the combined signal eigenvector $\mathbf{c}$ of $\mathbf{R}_\mathbf{x}^{fb}$.
3) Forward-backward averaging the sequence $\mathbf{c}$. The output k^{th} forward subsequence is $\mathbf{c}_k^f = \left[c_k \;\; c_{k+1} \;\dots\; c_{k+L_c-1}\right]^T$ and the output k^{th} backward subsequence is $\mathbf{c}_k^b = \left[c_{L_0-k+1}^* \;\; c_{L_0-1}^* \;\dots\; c_{L_0-L_c-k+2}^*\right]^T$ where L_c denotes the length of a subsequence. The correlation matrix of the forward-backward averaging on the combined eigenvectors is given by

$$\mathbf{R}_{\mathbf{c}}^{fb} = \frac{1}{K}\sum_{k=1}^{K}\left[\mathbf{c}_k^f \mathbf{c}_k^{f^H} + \mathbf{c}_k^b \mathbf{c}_k^{b^H}\right] \qquad (19)$$

where the number of subsequences is $K = L_0 - L_c + 1$.

4) Replace $\mathbf{R}_{\mathbf{c}}^{fb}$ to $\mathbf{R}_{\mathbf{x}}^{fb}$ in Eq. (10) and then perform the beamspace MUSIC.

The procedure first decorrelates the coherence by smoothing the covariance matrix of the received signal. After decorrelating, we generate a signal eigenvector, since eigenvectors of the smoothed covariance matrix is a linear combination of DOA vectors. To remove correlation perfectly, a spatial averaging is the third step. In step 4, calculate the covariance matrix of the signal eigenvector to replace that of received signal. Finally, the beamspace MUSIC can estimate the closely spaced DOAs of coherent sources.

7 Applications to BPSK and QPSK Demodulation

As shown in Fig. 4, we apply the proposed DOA estimation and the optimal beamformer to BPSK and QPSK transmissions. Denoting signals induced on all antenna elements as

$$\mathbf{x}(n) = [x_1(n)\ x_2(n)\ \ldots\ x_L(n)]_{L\times 1}^T \qquad (20)$$

and the weight vector of array system as

$$\mathbf{w} = [w_1\ w_2\ \ldots\ w_L]_{L\times 1}^T\ . \qquad (21)$$

The array system output becomes

$$y(n) = \mathbf{w}^H \mathbf{x}(n)\,. \qquad (22)$$

In the optimal beamformer, the weight vector is given by [2]

$$\mathbf{w} = \frac{1}{L}\mathbf{R}_{\mathbf{x}}^{-1}\mathbf{A}(\mathbf{A}^H\mathbf{R}_{\mathbf{x}}^{-1}\mathbf{A})^{-1}\mathbf{f} \qquad (23)$$

where $\mathbf{f}$ is an $M\times 1$ vector of all zeros except the first element equal to one and $|\mathbf{w}|^2 = \frac{1}{L}$.

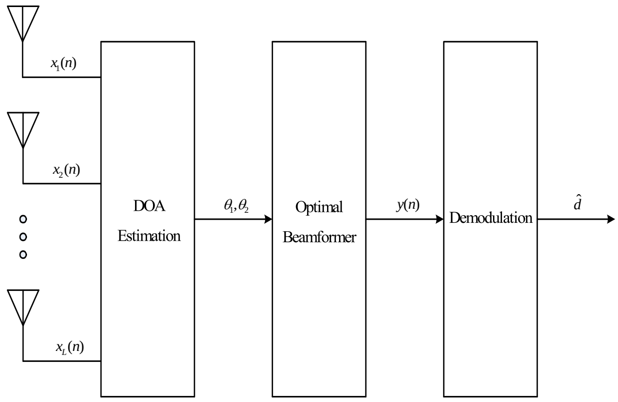

Fig. 4 Application of Improved beamspace MUSIC

7.1 Performance Analysis for BPSK

The BPSK signals can be modeled as [15]

$$\begin{aligned} s_1(n) &= \sqrt{p_s}\cos(\omega_s n) \qquad \text{for bit "1"} \\ s_2(n) &= -\sqrt{p_s}\cos(\omega_s n) \qquad \text{for bit "-1"} \end{aligned} \qquad (24)$$

where ω_s is a carrier frequency. Using Eq. (1), the received signal at the antenna array in Fig. 4 is given by

$$\begin{aligned}\mathbf{x}(n) &= \pm\sqrt{p_s}\cos(\omega_s n)\mathbf{a}(\theta_s) \\ &\quad + \sqrt{p_i}\left(\pm\delta^*\cos(\omega_s n) + \sqrt{1-|\delta|^2}\cos(\omega_i n)\right)\mathbf{a}(\theta_i) + \mathbf{n}(n). \end{aligned} \qquad (25)$$

The optimal beamformer can form a mainbeam at the desired DOA at θ_s and cancel the interference at the DOA at θ_i due to $\mathbf{w}^H\mathbf{a}(\theta_s) = 1$ and $\mathbf{w}^H\mathbf{a}(\theta_i) = 0$. Therefore, it yields the output of the beamformer as

$$\begin{aligned} y(n) &= \mathbf{w}^H\mathbf{x}(n) \\ &= \pm\sqrt{p_s}\cos(\omega_s n) + \mathbf{w}^H\mathbf{n}(n). \end{aligned} \qquad (26)$$

As illustrated in Fig. 5, $y(n)$ is demodulated by

$$
\begin{aligned}
z(n) &= \frac{2}{N}\cos(\omega_s n) y(n) \\
&= \frac{2}{N}\cos(\omega_s n)\left[\pm\sqrt{p_s}\cos(\omega_s n) + \mathbf{w}^H \mathbf{n}(n)\right] \\
&= \pm\frac{2}{N}\sqrt{p_s}\cos^2(\omega_s n) + \frac{2}{N}\cos(\omega_s n)\mathbf{w}^H \mathbf{n}(n) \\
&= \pm\frac{\sqrt{p_s}}{N} \pm \frac{\sqrt{p_s}}{N}\cos(2\omega_s n) + \frac{2}{N}\cos(\omega_s n)\mathbf{w}^H \mathbf{n}(n) \\
&= \pm\frac{\sqrt{p_s}}{N} \pm \frac{\sqrt{p_s}}{N}\cos(2\omega_s n) + \tilde{n}(n).
\end{aligned} \tag{27}
$$

The decision variable is

$$
\begin{aligned}
r &= \sum_{n=0}^{N-1} z(n) \\
&= \sum_{n=0}^{N-1} \pm\frac{\sqrt{p_s}}{N} \pm \sum_{n=0}^{N-1}\frac{\sqrt{p_s}}{N}\cos(2\omega_s n) + \sum_{n=0}^{N-1}\tilde{n}(n) \\
&= \pm\sqrt{p_s} + \tilde{n}.
\end{aligned} \tag{28}
$$

Approximately, $\sum_{n=0}^{N-1}\frac{\sqrt{p_s}}{N}\cos(2\omega_s n) = 0$ since a sum of cosine signal is zero if number of periods in the N samples is an integer.

The expected value of the decision variable is found by

$$
\begin{aligned}
E[r] &= E[\pm\sqrt{p_s} + \tilde{n}] \\
&= E\left[\pm\sqrt{p_s}\right] + E[\tilde{n}] \\
&= \pm\sqrt{p_s}.
\end{aligned} \tag{29}
$$

We have $E[\tilde{n}] = 0$ since $E[\mathbf{n}(n)] = 0$.
The variance of the decision variable is defined as

$$
Var[r] = E[r^2] - E^2[r] \tag{30}
$$

where

$$
\begin{aligned}
E[r^2] &= E[(\pm\sqrt{p_s} + \tilde{n})^2] \\
&= E[p_s \pm 2\sqrt{p_s}\tilde{n} + \tilde{n}^2] \\
&= E[p_s] \pm 2\sqrt{p_s}E[\tilde{n}] + E[\tilde{n}^2] \\
&= p_s + E[\tilde{n}^2].
\end{aligned} \tag{31}
$$

By using $\tilde{n} = \frac{2}{N}\sum_{n=0}^{N-1}\cos(\omega_s n)\mathbf{w}^H \mathbf{n}(n)$, we have

$$
\begin{aligned}
E[\tilde{n}^2] &= \frac{4}{N^2}\sum_{n=0}^{N-1}\sum_{m=0}^{N-1}\cos(\omega_s n)\cos(\omega_s m)\mathbf{w}^H E[\mathbf{n}(n)\mathbf{n}^H(m)]\mathbf{w} \\
&= \frac{4\sigma_n^2}{N^2}\sum_{n=0}^{N-1}\cos^2(\omega_s n)\mathbf{w}^H \mathbf{w} \\
&= \frac{2\sigma_n^2 |\mathbf{w}|^2}{N^2}\sum_{n=0}^{N-1}\left(1 + \cos(2\omega_s n)\right) \\
&= \frac{2}{N}\sigma_n^2 |\mathbf{w}|^2 .
\end{aligned} \tag{32}
$$

Substitute $E[\tilde{n}^2]$ and $E[r^2]$ into Eq. (30), the variance can be obtained as

$$
\begin{aligned}
Var[r] &= E[\tilde{n}^2] \\
&= \frac{2}{N}\sigma_n^2 |\mathbf{w}|^2 .
\end{aligned} \tag{33}
$$

We have $|\mathbf{w}|^2 = \frac{1}{L}$, then $Var[r] = \frac{2\sigma_n^2}{LN}$.
Using a beamformer before demodulation, the probability of bit error using BPSK modulation becomes [15]

$$
\begin{aligned}
P_{e,BPSK} &= Q\left(\frac{E[r]}{\sqrt{Var[r]/2}}\right) \\
&= Q\left(\sqrt{\frac{Lp_s N}{\sigma_n^2}}\right) \\
&= Q\left(\sqrt{\frac{2LE_b}{N_0}}\right)
\end{aligned} \tag{34}
$$

where $E_b = p_s N$ is energy per bit and $N_0 = 2\sigma_n^2$.
The Q - function is defined as

$$
Q(x) = \frac{1}{\sqrt{2\pi}}\int_x^\infty e^{-\frac{z^2}{2}} dz . \tag{35}
$$

Without a beamformer (no array), the probability of bit error is $P_{e,BPSK} = Q\left(\sqrt{\frac{2E_b}{N_0}}\right)$. This indicates that if we use a beamformer before demodulation, the probability of bit error decreases due to the gained L times of energy per bit.

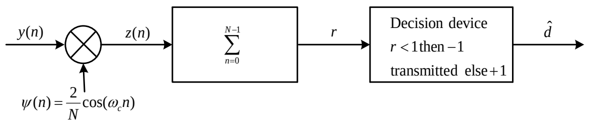

Fig. 5 BPSK demodulation

7.2 Performance Analysis for QPSK

Using the demodulator shown in Fig. 6, the probability of symbol error rate is

$$P_{e,QPSK} = 1 - P_c \tag{36}$$

where P_c denotes the probability which both two bits of a symbol are correctly detected given as

$$P_c = \left(1 - P_{e,BPSK}\right)^2 \tag{37}$$

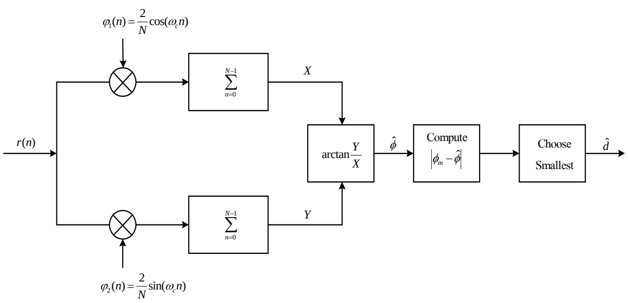

Fig. 6 QPSK demodulation

8 Simulation Results

We illustrate the performance of the proposed algorithm referring as (FBCA BMUSIC = Forward-backward spatial smoothing, combined signal eigenvector averaging, beamspace MUSIC) in comparison to

1. MUSIC
2. FB MUSIC = Forward-backward spatial smoothing, MUSIC
3. CFBA MUSIC = Combined signal eigenvector, forward-backward averaging, MUSIC
4. BMUSIC = Beamspace MUSIC
5. FB BMUSIC = Forward-backward spatial smoothing, beamspace MUSIC
6. CFBA BMUSIC = Combined signal eigenvector, forward-backward averaging, beamspace MUSIC

Consider two coherent sources with DOAs at $\theta_s = -1^\circ$, $\theta_i = 1^\circ$ and correlation coefficient $\delta = 0.8e^{j\frac{\pi}{4}}$ impinging on an array of $L = 21$ elements. It is divided into $K = 6$ subarrays. The number of snapshots is $N = 100$. The signal to noise ratio defined as $SNR = 10\log_{10}(\sigma_n^{-2})$ is 10 dB. In the beamspace MUSIC, the five main beams are expected at $B = \{-8^\circ, -1^\circ, 1^\circ, 6^\circ, 10^\circ\}$ as plotted in Fig. 7. Fig. 8 forms other five expected beams at $B = \{-8^\circ, -0.5^\circ, 0.5^\circ, 6^\circ, 10^\circ\}$. When the DOAs become closer, the DOA estimation based on either MUSIC or BMUSIC is improved if we use the proposed procedure (FBCA BMUSIC) as shown in Figs. 9-10. The FBCA BMUSIC gives the most accurate estimation with high separated magnitudes.

Moreover, the performance is evaluated in terms of mean squared errors (MSEs) [16] versus (1) magnitude of correlation coefficients, (2) noise variances and (3) SNRs. The mean squared errors between the actual and estimated DOAs are averaged by 100 Monte Carlo trials at each fix correlation value or noise variance or SNR. As the magnitude of absolute correlation value approaches to one, the signal sources are fully correlated. Accordingly, the errors are increased as the correlation coefficient increases as seen in Fig. 11(a)-(b). Fig. 11(a) shows the MSEs of the estimated DOA for $\theta_s = -1^\circ$ while Fig. 11(b) shows the MSEs of the estimated DOA for $\theta_i = 1^\circ$. The FBCA BMUSIC outperforms than others. The MSEs illustrated in Figs. 12(a)-(b) varies to noise variances whereas the MSEs illustrated in Figs. 13(a)-(b) varies to SNRs. The error is the more or less 1°, if the noise variance increases or the SNR decrease. However, using the proposed estimation method, FBCA BMUSIC, reduces the estimation errors. Among three evaluations, the proposed algorithm can improve the angular resolution of the beamspace MUSIC. Also, the probability of resolution is the highest than other methods in low SNRs as plotted in Fig. 14. To show capability of the improved angular resolution, three DOA estimates at -3°, 0° and 3° can be well separated by the proposed FBCA BMUSIC method.

For bit error rate (BER) and symbol error rate (SER) evaluations, using the proposed FBCA BMUSIC method can achieve less errors. For both BPSK and QPSK, The application of the proposed DOA estimation can reduce BER and SER of the conventional demodulation (no array) as shown in Figs. 16-17, respectively. Fig. 18 shows a comparison between simulation results and analytic formulas of probability of bit errors using BPSK modulation given in Eq. (34). The analytic result is less than the simulation result due to the approximation. For QPSK modulation, the comparison is shown in Fig. 19 which Eq. (36) is used to compute the probability of symbol errors. The results are similar to that of BPSK transmission.

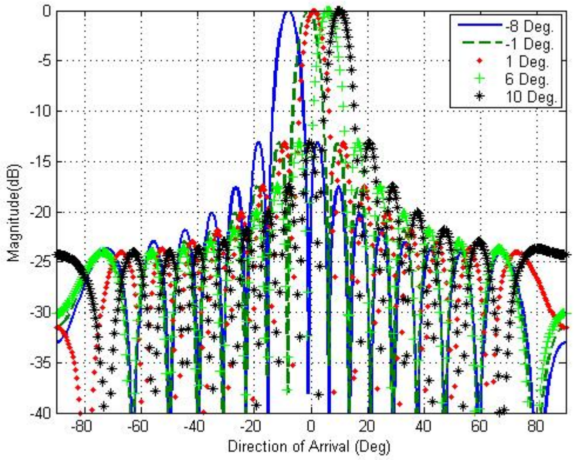

Fig. 7 Beamforming of expected DOAs at $B = \{-8^\circ, -1^\circ, 1^\circ, 6^\circ, 10^\circ\}$

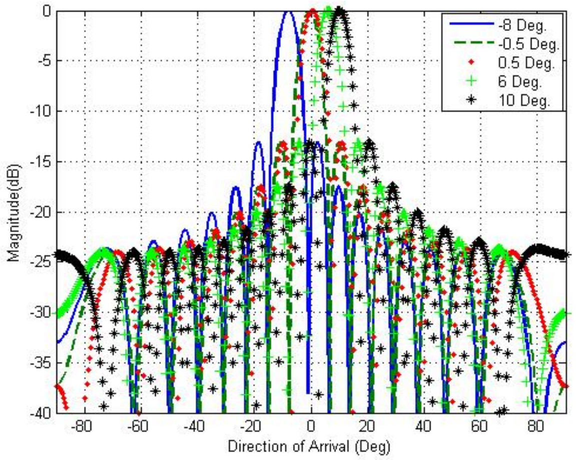

Fig. 8 Beamforming of expected DOAs at $B = \{-8^\circ, -0.5^\circ, 0.5^\circ, 6^\circ, 10^\circ\}$

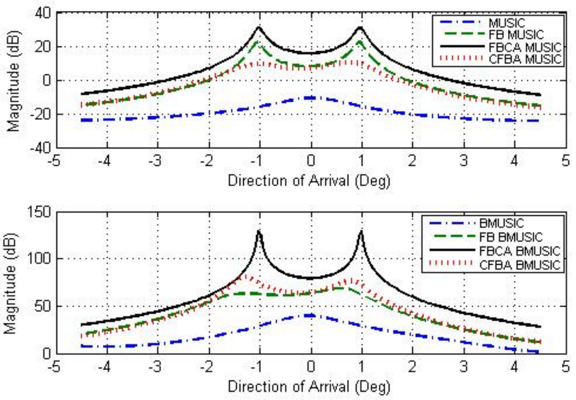

Fig. 9 DOA estimation at -1° and 1°

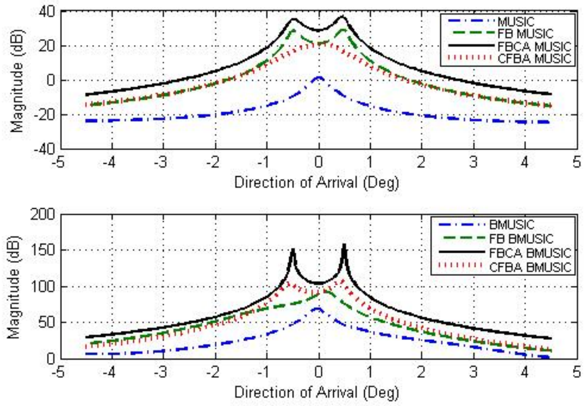

Fig. 10 DOA estimation at -0.5° and 0.5°

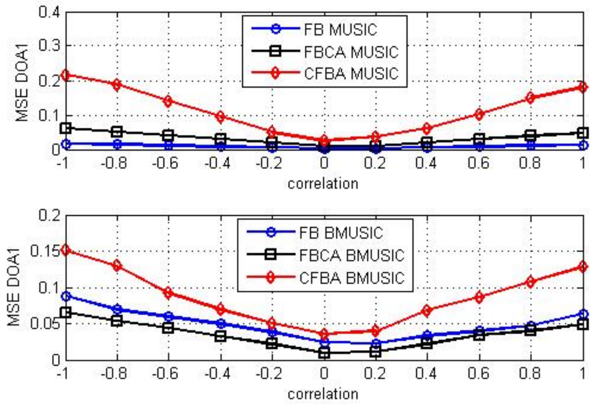

(a)

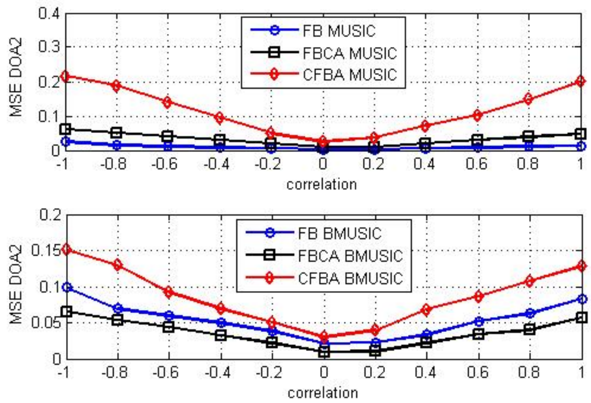

(b)

Fig. 11 MSE versus correlation (a) $\theta_s = -1^\circ$ (b) $\theta_i = 1^\circ$

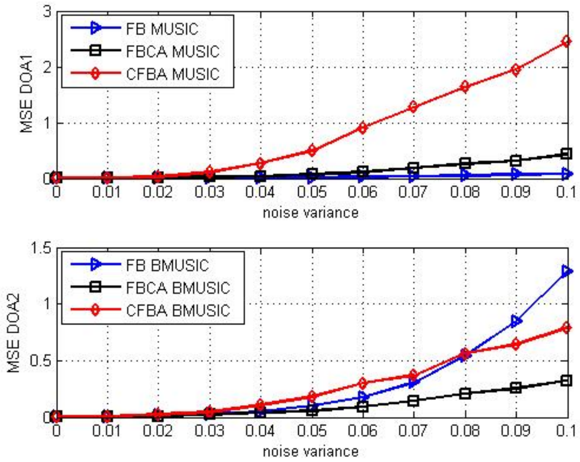

(a)

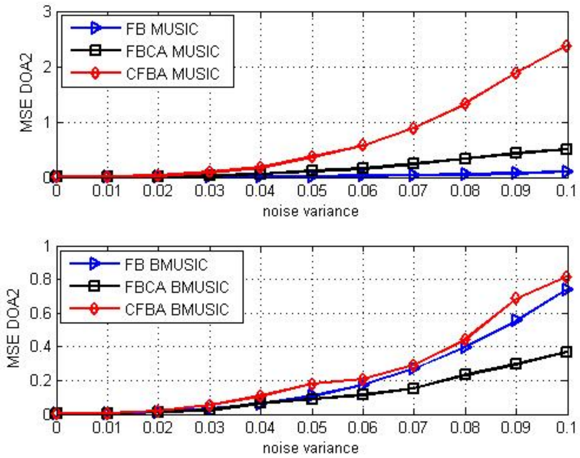

(b)

Fig. 12 MSE versus noise variance (a) $\theta_s = -1^\circ$ (b) $\theta_i = 1^\circ$

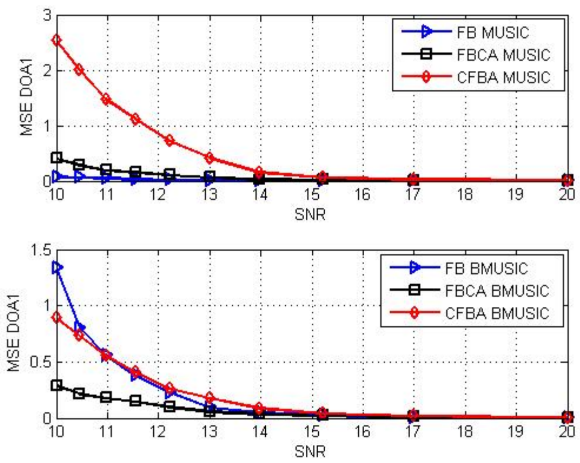

(a)

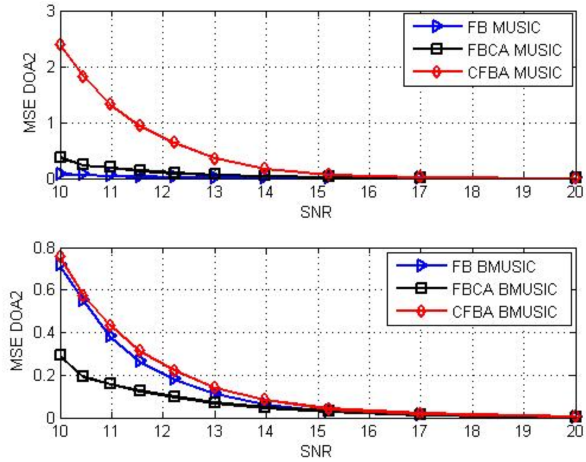

(b)

Fig. 13 MSE versus SNR (a) $\theta_s = -1^\circ$ (b) $\theta_i = 1^\circ$

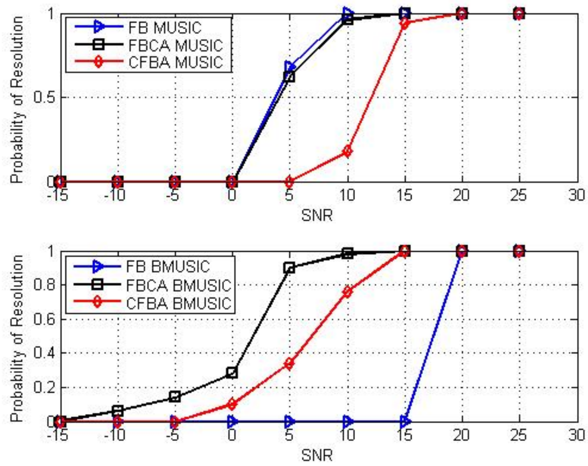

Fig. 14 Probability of Resolution versus SNR

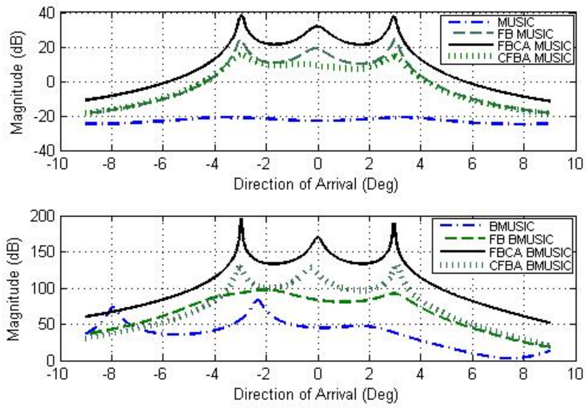

Fig. 15 DOA estimation at $-3^\circ, 0^\circ$ and 3°

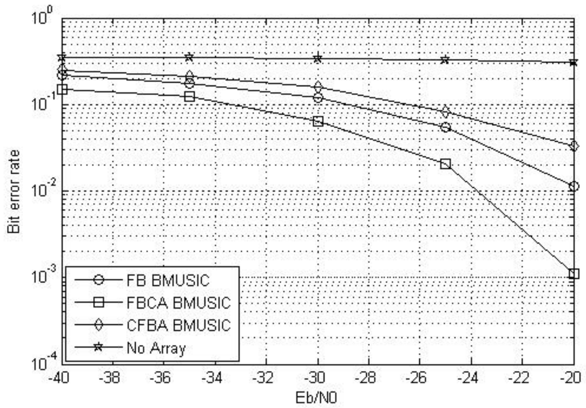

Fig. 16 Bit error rate (BPSK)

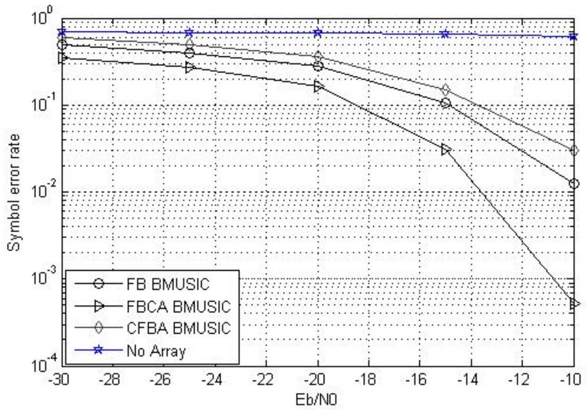

Fig. 17 Symbol error rate (QPSK)

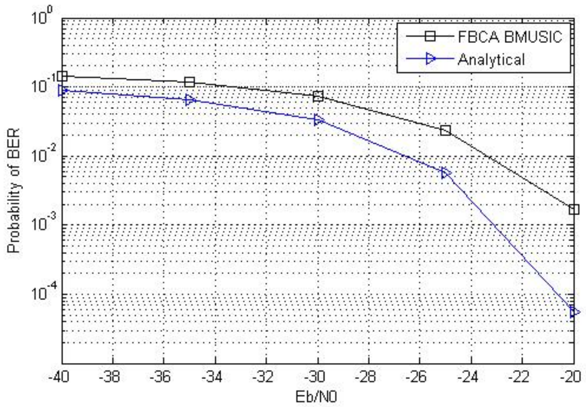

Fig. 18 Probability of bit errors (BPSK)

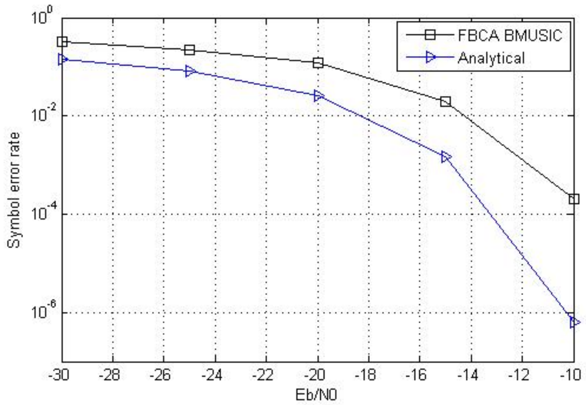

Fig. 19 Probability of symbol errors (QPSK)

9 Conclusion

An improved angular resolution of beamspace MUSIC is presented for finding directions of coherent sources. Decorrelation is achieved by forward-backward spatial smoothing. Combined signal eigenvectors are generated as a virtual received signal. Forward-backward averaging is used to smooth the combined signal sequence. After decorrelating the coherent incident waveforms, the beamspace MUSIC can distinguish closely space directions. It is applied to BPSK and QPSK demodulation which able to decrease BERs and SERs as well.

References:

[1] S. Santosh, O. P. Sahu and M. Aggarwal, An Overview of Different Wideband Direction of Arrival (DOA) Estimation Methods, *WSEAS Transactions on Signal Processing*, Vol. 5, Issue 1, Jan 2009, pp. 11-22.

[2] C. L. Godara, *Smart Antennas*, CRC press, 2004.

[3] P. Stoica and A. Nehorai, Comparative Performance Study of Element-space MUSIC and Beam-space MUSIC Estimators, *Springer: Circuit, System and Signal Processing*, Vol. 10, No. 3, 1991, pp. 285-292.

[4] S. U. Pillai and B. H. Kwon, Forward/backward Spatial Smoothing Techniques for Coherent Signal Identification, *IEEE Transactions on Acoustics, Speech, and Signal Processing*, Vol. 37, No. 1, Jan. 1989, pp. 8-15.

[5] Y. Yang, C. Wan, C. Sun and Q. Wang, DOA Estimation for Coherent Sources in Beamspace Using Spatial Smoothing, *4th International Conference on Information, Communications and Signal Processing*, Vol. 2, Dec. 2003, pp. 1028-1032.

[6] J. Li, Improved Angular Resolution for Spatial Smoothing Techniques, *IEEE Transactions on Signal Processing*, Vol. 40, No. 12, Dec. 1992, pp. 3078-3081.

[7] D. A. Linebarger, R. D. DeGroat and E. M. Dowling, Constrained Beamspace MUSIC, *IEEE International Conference on Acoustics, Speech and Signal Processing*, Vol. 4, Apr. 1993, pp. 548-551.

[8] H. B. Lee and M. S. Wengrovitz, Beamformer Preprocessing for Enhanced Resolution by the MUSIC Algorithm, *5th ASSP Workshop on Spectrum Estimation and Modeling*, Oct. 1990, pp. 149-153.

[9] H. B. Lee and M. S. Wengrovitz, Resolution Threshold of Beamspace MUSIC for two Closely Spaced Emitters, *IEEE Transactions on Acoustics, Speech, and Signal Processing*, Vol. 38, No. 9, Sep. 1990, pp. 1545-1559.
[10] V. I. Vasylyshyn, Antenna Array Signal Processing with High-Resolution by Modified Beamspace MUSIC Algorithm, *6th International Conference on Antenna Theory and Techniques*, Sep. 2007, pp. 455-457.
[11] J. A. Cadzow, A High Resolution Direction-of-Arrival Algorithm for Narrow-band Coherent and Incoherent Sources, *IEEE Transactions on Acoustics, Speech, and Signal Processing*, Vol. 36, No. 7, Jul. 1988, pp. 965-979.
[12] N. Odachi, H. Shoki and Y. Suzuki, High-speed DOA Estimation using Beamspace MUSIC, *IEEE 51st Vehicular Technology Conference*, 2000, pp. 1050-1054.
[13] P. Totalong and A. El-Jaroudi, Robust High-Resolution Direction-of-Arrival Estimation via Signal Eigenvector Domain, *IEEE Journal of Oceanic Engineering*, Vol. 18, No. 4, Oct. 1993, pp. 491-499.
[14] R. Suleesathira, Close Directions of Arrival Estimation for Multiple Narrowband Sources, *7th International Conference on Signal Processing and Its Applications*, Vol. 2, Jul. 2003, pp. 403-406.
[15] J. G. Proakis, *Digital Communications*, McGraw Hill, 2000.
[16] P. Palanisamy, N. Kalanasundaram and A. Raghunandan, A New DOA Estimation Algorithm for Wideband Signals in the Presence of Unknown Spatially Correlated Noise, *Signal Processing*, Vol. 89, Issue 10, 2009, pp. 1921-1931.